Investigation of Nb-doped NASICON Solid Electrolyte

A Dissertation for
Course code and Course Title:PHY 651
Dissertation Credits: 16
Submitted in partial fulfillment of Masters Degree

M.Sc in Solid State Physics

by

Kartik Faldessai
Seat number:22P0430014
ABC ID:312826108754
PRN:201905580

Under the supervision of
DR.BHOLANATH PAHARI

School Of Physical and Applied Science
Physics discipline

Goa University
May 2024

Examined by:

Seal of the School

1

DECLARATION BY STUDENT

I hereby declare that the data presented in this Dissertation report entitled, "Investigation of Nb-doped NASICON Solid Electrolyte" is based on the results of investigations carried out by me in the Physics Discipline at the School of Physical and Applied Sciences, Goa University under the Supervision of Dr. Bholanath Pahari and the same has not been submitted elsewhere for the award of a degree or diploma by me. Further, I understand that Goa University or its authorities will be not be responsible for the correctness of observations / experimental or other findings given the dissertation. I hereby authorize the University authorities to upload this dissertation on the dissertation repository or anywhere else as the UGC regulations demand and make it available to any one as needed.

Name: Mr. Kartik Faldessai

Roll no: 22P0430014

Discipline: Physics

School of Physical and Applied Sciences

Date: 08|05|2024
Place: Goa University

COMPLETION CERTIFICATE

This is to certify that the dissertation "Investigation of Nb Doped NASICON solid electrolyte" is a bonafide work carried out by Mr. Kartik Faldessai under my supervision in partial fulfilment of the requirements for the award of the degree of M.Sc in Physics at the School of Physical and Applied Sciences, Goa University.

Supervisor: Dr. Bholanath Pahari

Physics

Date: 08/05/2024

Dean: Prof. Ramesh. V. Pai

Physics

School of Physical and Applied Sciences

Date:

Place: Goa University

School stamp

3

Contents

1 Introduction

1.1 Secondary storage devices

Majority of conventional energy sources uses a large amount of Fossil fuels which leads to emission of green house gas which has significant negative impacts on the environment. Solar, wind and hydro energy are one of the best alternative to tackle this problem as they are environment friendly and have immense potential for renewable energy generation. Yet its irregularities and inability to be controlled are some of the main issues that needs to be resolved for the widespread use of these sources in place of conventional energy sources. Use of energy storage devices such as batteries can help in storing the energy from these sources and help in large-scale adoption of these alternative energy sources.[1] Here are some of the secondary storage systems:

1.1.1 Lithium ion batteries

Li-ion batteries are one of the most popular battery which is used widely mainly due to their high power and energy density which makes them useful for portable electronics and electronic vehicles. It has some advantages due to use of lithium, as among other elements it has incredibly low reduction potential which helps it to achieve its full cell potential, also it has the smallest radii and is third lightest element which helps it to have high power density and volumetric capacity. It mainly uses intercalation cathode material such as transition metal and graphite as anode.[2]

1.1.2 Lithium oxygen batteries

Li-oxygen batteries can provide a specific energy output which is 3-4 times greater than that of existing lithium ion batteries, using oxygen from the environment and metal lithium electrodes which has a high capacity. To achieve the full potential of Li oxygen batteries it must operate in ambient atmospheric conditions, research is to be done as how the atomspheric contaminants such as H_2O and CO_2 affect the cathode. These common air impurities react with conventional discharge product of Li_2O_2, forming $LiOH$ and Li_2CO_3 complicating the fundamental $Li-O_2$ electrochemistry by requiring higher charge potentials for decomposition. Which reduces the overall efficiency and lifespan of battery.[3]

1.1.3 Zinc air batteries

The zinc-air batteries provides a secure, eco-friendly, and potentially cost-effective and straight-forward way of storing and supplying electrical energy for portable and stationary devices, which includes the electric vehicles. Zinc air batteries are of mainly of three types, Primary (can only be used once), secondary(electrically rechargeable) and fuel cells. Zinc is a safer metal when it is compared to lithium and therefore it can be fully recycled. Also zinc is abundantly available in nature. A zinc-air battery has three primary parts: a zinc anode, an alkaline electrolyte (KOH), and an air cathode, Which is generally made of porous carbon material.[4]

1.1.4 Aluminium ion batteries

The cost of aluminium ion batteries is low as aluminum is abundantly found in nature and it has high volumetric capacity more than 5-7 times that of sodium and lithium. Research is going on the aluminium ion batteries there are three major reasons. Firstly aluminium is comparatively easy to handle in ambient environment and it offer significant safety improvements for this kind of battery. Secondly three redox electrons can be exchanged per cation in aluminium therefore inserting one Al^{3+} has the same effect as adding three Li^+ ions in traditionally intercalation cathodes. Also it posses a higher volumetric capacity than Li, Na, K, Mg, Ca due to its high density (2.7 g cm^3 at room temperature) therefore the energy stored in aluminium ion batteries on a per volume basis is higher than that in other metal based batteries.[5]

1.1.5 Sodium ion battery

In sodium ion battery Na^+ ions move through the cathode during charging, Intercalating into the anode, and vice versa during the discharge. Carrier the cathode material that can be used in sodium ion batteries are organic material, transition metal oxides, and phosphates. The anode material that can be used are graphite material, sulphides organic compounds and selective carbonic materials.

Here charging and discharging process of sodium ion battery is shown in the left portion of the image comprising of the components such as the cathode ($NaMnO_2$), anode (hard carbon), electrolyte, and current collectors. Whereas on the right side of the figure, the chemical reactions
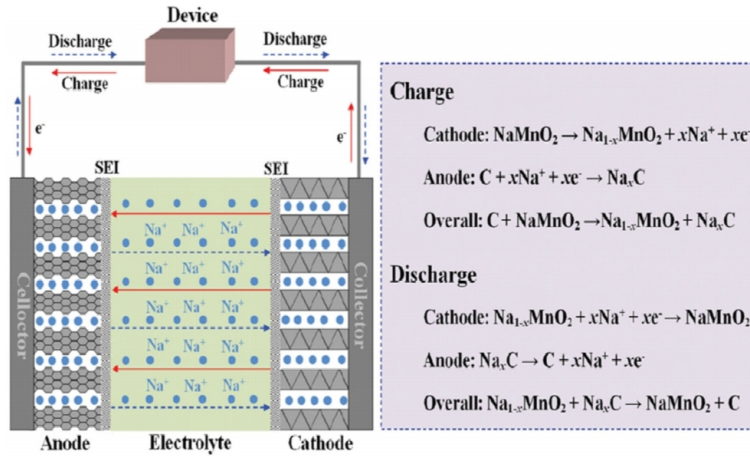
Figure 1: Schematic diagram Sodium-ion battery and it's reaction[6]

which are occurring at both electrodes and redox reactions in a $NaMnO_2$ based cathode and carbon-based anode system are displayed.[7]

1.2 Need for Sodium ion batteries

Lithium ion batteries are one of the most widely used batteries mainly due to their high energy density and long life that is mostly used in electronic vehicles and portable devices, However the due to shortage of lithium salt resources it is difficult to keep up with the growing lithium ion battery demands therefore there is a need to find an alternative energy storage secondary device which is similar to that of lithium ion battery. Sodium ion battery is a good alternative to lithium ion battery as they have a similar working mechanism and performance also sodium is also abundantly found in nature. Like lithium-ion batteries, traditional liquid sodium-ion batteries pose a safety risk. These risks include leaks, fires, and explosions due to the flammable organic liquids used in their electrolytes. To make sodium-ion batteries truly practical for large-scale applications, researchers need to develop safe, solid electrolyte materials which is both safer and has high ionic conductivity.[8]

1.3 Solid electrolyte in sodium ion battery

The effectiveness of batteries especially sodium ion battery relies heavily on the ionic conductivity of electrolyte. Solid electrolytes simplifies the design of battery by removing extra separator components, often resulting in improved system stability. Here are some of the solid electrolyte that can be used in sodium ion batteries

- **Sulfide-based inorganic electrolyte**

  Sulfide-based inorganic electrolytes, such as Na_3PS_4, facilitate rapid Na-ion conduction at ambient temperatures and it can be produced at a lower temperature. Na_3PS_4 has a notable room temperature conductivity (10^{-4} S/cm) and features a broad electrochemical window of 5 V. The glass-ceramic form of Na_3PS_4 shows even higher total ionic conductivity, ranging from 2.0 to 4.6×10^{-4} S/cm at the room temperature, along with a reduced activation energy for hopping, between 19 and 27 kJ/mol. The sulfide electrolyte generally has poor chemical stability as they react with moisture in air. Phosphorus in the solid electrolytes based on Na_3PS_4 is prone to instability when exposed to oxygen in the atmosphere. Additionally, inorganic electrolyte materials based on sulfides have a tendency to decompose due to hydrolysis caused by moisture in the air therefore its chemical stability need to be enhanced. The production cost of sulphide electrolyte battery is low as cold pressing treatment is enough for good contact between electrolyte and electrode materials.

- **β-Alumina**

  It is one of the first fast ion conductor which was utilized in commercial Na–S and Na-metal chloride batteries, mainly used at high temperatures (300 °C). It only shows ion conductivity along its conduction plane and shows zero conductivity in vertical direction. It has two different types of crystal structure, the β-alumina phase $Na_2O_{11}Al_2O_3$, which shows hexagonal symmetry (P6$_3$/mmc)and the β"-alumina phase ($Na_2O_5Al_2O_3$), which shows a rhombohedral symmetry. The rhombohedral β"-alumina phase has a higher concentration of Na ions within the conduction plane and has a bigger unit cell, which is 1.5 times longer than the of the β-alumina phase along c-axis.
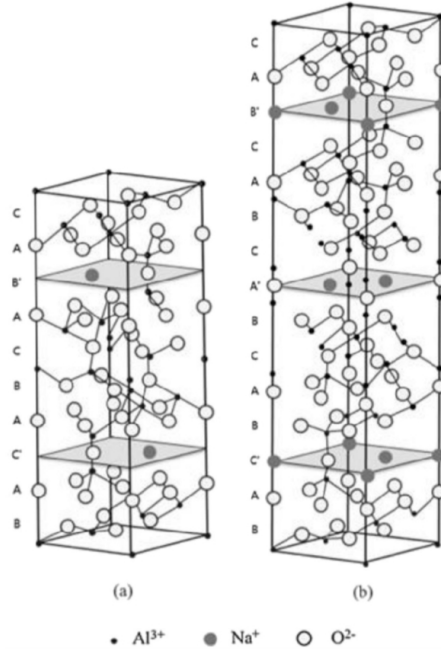
Figure 2: (a) Na$^+$$\beta$-alumina and (b) Na$^+$$\beta$"-alumina [6]

- **Organic polymer electrolyte**

  There are two types of organic polymer electrolyte gel polymer electrolyte and solvent free solid electrolyte gel polymer electrolyte has a higher conductivity(10^{-3} S/cm at room temperature) but it has weaker mechanical properties as compared to solvent free electrolyte. In comparison to gel electrolyte the solvent-free polymer electrolyte exhibits significantly lower ionic conductivity, ranging only between 10^{-9} to 10^{-6} S/cm at room temperature. The gel functions similarly to that of a liquid electrolyte therefore like the liquid electrolyte it also has some safety issues where as solvent free solid electrolyte had good mechanical properties. The ionic conductivity of PVdF-HFP(Poly(vinylidenefluoride-co-hexafluoropropylene) gel polymer electrolyte is roughly 2.4×10^-3 S/cm, with a transference number of roughly 0.3. PVdF-HFP/Glass Fiber NaClO$_4$-PC room temperature conductivity is 4.60×10^{-3} S/cm [6]

1.4 NASICON Solid electrolyte

1.4.1 History

In the early 1980s, research on NASICON solid-state electrolytes mainly centered around discovering novel materials and reviewing their crystal structures. By the 1990s, the emphasis shifted towards enhancing conductivity through methods like doping with low-valence elements or incorporating additives. However, between 2000 and 2010, the interest decreased, and progress came to a halt. Since 2010, there has been a resurgence in NASICON research with a significant focus on improving interfaces between the cathode/electrolyte or metal anode/electrolyte, as well as exploring new battery structure. In 1976, the synthesis and study of the crystal structure of a material with chemical formula $Na_{1+x}Zr_2Si_xP_{3-x}O_{12}$ was done by Goodenough and Hong, along with others . They found out that making dense of $Na_{1+x}Zr_2P_{3-x}Si_xO_{12}$ was easier as compared to β"-alumina. Goodenough and his colleagues first introduced the term "NASICON".

1.4.2 Structure

The NASICON framework shows significant variations due to its capacity to incorporate varying stoichometric compositions given by the formula $Na_{1+x}Zr_2Si_xP_{3-x}O_{12}$, where x ranges from 0 to 3.At room temperature (RT), NASICON takes a rhombohedral crystalline structure with a space group of R-3c when the content of Si ranges from $0 < x < 1.8$.

As the Si content increases to $1.8 < x < 2.3$, it experiences a transformation to a monoclinic symmetry with the C2/c space group. As the Si content is further increased, it returns to the rhombohedral R-3c form. . It can again convert into rhombohedral phase from monoclinic phase due
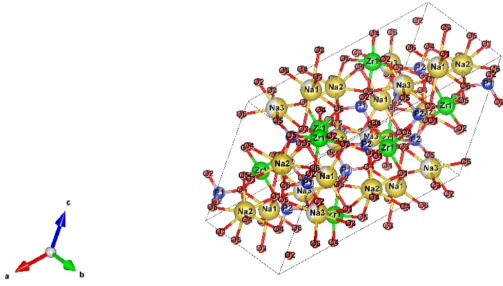
Figure 3: Monoclinic
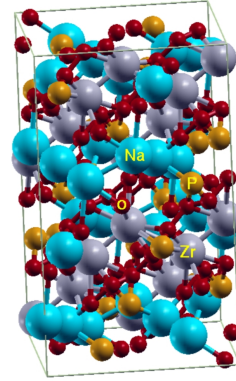
Figure 4: Rhombhhedral

to the deformation of the unit cell which occurs at 420-450K.[9] In NASICON's three-dimensional framework, the ZrO_6 octahedra and PO_4 tetrahedra share corners, creating interconnected channels where sodium ions can move.

In the rhombohedral phase, sodium ions migrate from Na(1) sites to Na(2) sites, while in the monoclinic phase, they travel to Na(2)/Na(3) sites. Compared to the rhombohedral phase, the monoclinic phase offers an additional migration channel and generates more vacant sites, facilitating sodium ion movement. [6]

1.4.3 Properties

NASICON's crystalline structure has three-dimensional tunnels that enable the movement of sodium ions within the material. The strong structure of NASICON material has a great practical use and it posses high thermal and chemical stability in different environments. The ionic conductivity of NASICON electrolytes can vary significantly depending on factors such as chemical composition, phase structure lattice parameters and sodium concentration. This is due to the different interactions between mobile ions and skeleton atoms.[6] For practical use of NASICON electrolyte it should have sufficiently high ionic conductivity ($> 10^{-3}$ Scm^{-1}) and high critical current density(1.0 mA cm^2). The $Na_3Zr_2Si_2PO_{12}$ electrolyte exhibits relatively low room temperature ionic conductivity, approximately 10^{-4} $S\,cm^{-1}$, and a constructed sodium battery is constrained to a operate at a low cycling

current density between 0.1 to 0.25 mA cm^{-2}. The Mg^{2+} substituted $Na_{3.4}Mg_{0.1}Zr_{1.9}Si_{2.2}P_{0.8}O_{12}$ electrolyte shows impressive properties, including high room temperature ionic conductivity conductivity of 3.6×10^{-3} S cm^{-1} and a wide electrochemical window extending up to 6 V.[10] The highest conductivity of Sc and Ge co-doped NASICON electrolyte with a high ionic conductivity of 4.64 10^{-3} S cm^{-1} was obtained for the $Na_{3.125}Zr_{1.75}Sc_{0.125}Ge_{0.125}Si_2PO_{12}$ structure.[11]

The materials $Na_{3.3}Zr_{1.9}Nb_{0.1}Si_{2.4}P_{0.6}O_{12}$, $Na_{3.4}Sc_{0.4}Zr_{1.6}Si_2P_{0.6}O_{12}$, $Na_{3.3}La_{0.3}Zr_{1.7}Si_2PO_{12}$, and $Na_{3.4}Zr_2Si_{2.4}P_{0.6}O_{12}$ exhibit good total conductivity, with values of approximately 4.0 mS/cm, 3.4 mS/cm, and 5.0 mS/cm at 25 °C, respectively and $Na_{3.3}Zr_{1.9}Nb_{0.1}Si_{2.4}P_{0.6}O_{12}$ has a conductivity value, reaching up to 5.51 mS/cm. [8] The chemical stability of ceramic electrolytes is crucial for their performance in batteries. Despite achieving low ionic resistivities they often degrade and develop cracks when exposed to molten sodium at temperatures around 300 °C.[12]

1.4.4 Challenges

While there are many Advantages of using NASICON material as solid electrolyte, there are many problems which needs to be adressed. Here are some of the challenges

1.4.5 Ionic conductivity at room temperature

The benchmark for a good ionic conductivity is 10^{-3} Scm^{-1}, and to use NASICON solid electrolyte on a large scale the ionic conductivity should be higher than this, but generally ionic conductivity is lower than this in NASICON material. Therfore it is a necessity to increase conductivity of the NASICON material at room temperature.

1.4.6 The interfacial resistance

Batteries which have solid electrolyte faces poor contact at the electrode electrolyte interface. Due to poor contact the interfactial resistance is large as the movement of Na^+ ions is hindered which can lead to premature shortcircuit of the batteries.[13]

1.4.7 Impurities

Many impurities are formed during the synthesis of NASICON material which leads to mechanical weakness and lowers the ionic conductivity. The primary impurity that is formed during synthesis is monoclinic ZrO_2 phase which may lower the ionic conductivity of the electrolyte. It has been found out that the ionic conductivity of zirconia free NZSPs is 3.49 mS cm^{-1} and a bulk conductivity of 10 mS cm^{-1} at room temperature which makes it ideal for solid state battery application. Tests also shows that it has a significantly better performance. Therfore the synthesis of NZSPs should be optimized to prevent formation of impurities. [13]

1.5 Objective

NASICON material with Na-Content per formula unit of 3.4 are reported to display highest Na-ion conductivity. We thus plan to synthesize NASICON material with general formula $Na_{3.4-x}Zr_{2-x}Nb_xSi_{2.4}P_{0.6}O_{12}$ with x=0, 0.1. Phase purity and crystal struture of the prepared compound will be determined by X-ray diffraction technique. Electrical properties of the sample will be measured by Impedence spectroscopy. Ionic transference number will be calculated will be calculated by DC polarization technique.

2   Expiermental section

2.1   Sample Preparation

A NASICON solid electrolytes were synthesized by solution-assisted solid state reaction method. we used $NaNO_3$, $ZrO(NO_3)$, Nb_2O_5, $Si(OCH_2CH_3)_4$, and $NH_4H_2PO_4$ as raw materials for synthesis of the two samples. First, stoichometric amounts of $ZrO(NO_3)_2$ and $NaNO_3$ were mixed and dissolved in deionized water. When the solution was clarified, an appropriate amount of HNO_3 solution was added and it was stirred for 5 h the acid helps to dissolve the precursor homogeneously. When a clear solution was reached again, $Si(OCH_2CH_3)_4$, and Nb_2O_5 were added. For the synthesis of second sample (Nb doped), Nb_2O_5 was as added during this step. Then after stirring continuously for 1 hr, a white suspension was obtained. The obtained suspension was kept for overnight stirring and then was dried in an oven at 80 °C for 24 h. The resulting powder was then ground with the

Figure 5: Mortar and pastle used for grinding

help of a mortar and a pastle by hand for 6 h so that it mixes properly and then calcined in a muffle furnace at 800 °C for 12 h, Calcination removes water/solvents which may be present. It initiates NASICON formation, and also it improves crystallinity for better conductivity, the calcination temperature and time period for which the sample is calcined is crucial to form a sample with minimal impurities. After calcination the resulted white color powder was finally pressed into discs at room temperature using a stainless steel cylindrical mold with a diameter of 10 mm under 3

tons pressure for 2 minutes. NZSP or NZNSPx samples were then sintered at 1260 °C. Sintering further helps to increase the density of NASICON material, potentially improving conductivity and strength. It can also promote grain growth for more efficient ion transport pathways. For X-ray analysis sintered pellets were grinded and fine power was used whereas AC and DC conductivity measurements were carried out with the help of sintered pellets.

2.2 Characterization techniques

Three characterization techniques were used to analyse the sample firstly phase identification was carried out by Powder Xrd, Ionic conductivity was measured by impedence spectroscopy and DC polarization was used to find the ionic transference number here is a breif description of these techniques:

2.2.1 X-ray diffraction

X-ray diffraction method is one of the most widely used technique to analyse the crystal structure and the atomic spacing. It relies on constructive interference of monochromatic X-rays with crystalline sample.

Figure 6: X-ray diffractometer (XRD)

X-rays which are generated by a cathode ray tube, are first filtered so that it gives monochro-

matic radiation, and are then collimated so that the X-rays are concentrated, then these are directed towards the sample. A constructive interference (and a diffracted ray) occurs when the interaction between incoming ray's and the sample fulfills the Braggs's law:

$$n\lambda = 2dsin\theta$$

Where n represent an integer, λ is the X-ray wavelength, the interplanar spacing causing diffraction is given by d and θ is diffraction angle. The X-rays which are diffraction are detected, processed and then counted. By rotating the sample across 2θ range all potential diffraction direction of lattice are observed. Then by converting the diffraction peaks at different angles to d-spacings helps to identify the compound by comparing the observed d-spacings with standard reference pattern. Crystal structure of different materials can be found out by using specialized techniques such as Reitveild refinement. [14]

- **Principle**

  In X-ray diffraction (XRD), the electrons are emmited by a heating a tungsten filament within a vaccume. These electrons are then subjected to a high potential field and then guided towards a target material, which leads to the emission of X-rays.
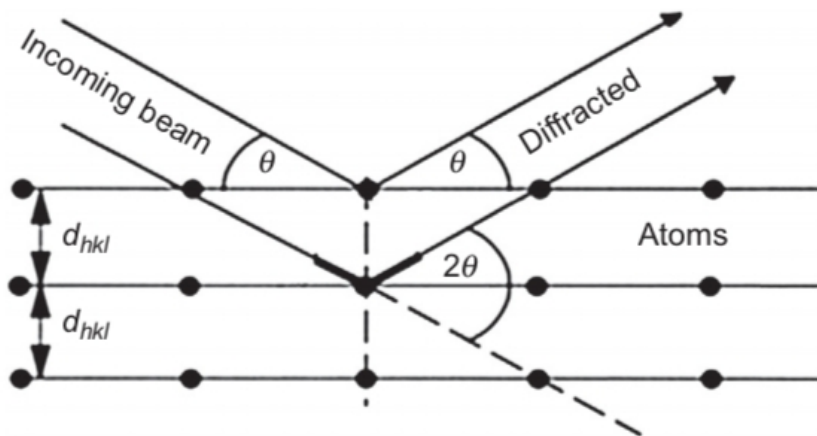
Figure 7: Geometrical condition for diffraction from lattice planes

15

When X-rays are made incident on matter various interaction occurs resulting in different absorption and scattering effects. There is a periodic arrangement of atoms in crystalline materials when X-rays encounter the atomic plane, they are then diffracted at different angles based on the wavelength of incident beam and spacing between atomic spaces. These patterns can be observed to find the crystal structure of different materials.

Instrumentation

X-ray diffractometers presently are controlled by computers and have varying hardware depending upon their intended use here are some of the important parts.

- **X-ray source**

  The two important factors influencing the X-ray production are the radiations intensity and shape/size of beam which is coming out from the anode. To produce X-ray photons, it is necessary to accelerate electrons emmitied from the tungsten filament. Typically, voltages ranging from 20-60 KV are employed. During the generation of X-rays maximum energy is given out as heat and only 1 percent is used for production of the radiation, therefore continues water cooling of anode is required.

- **Ganiometer**

  It is one of the main parts of the diffractometer allowing precise movement of X-ray source, sample and the detector in reference to eachother. For all angles θ the distance between the detector and the sample remains constant. Two common types of ganioneter are widely used θ/θ , in this kind of ganioneter the sample remains fixed and X-ray source and detector moves and $\theta/2\theta$ wherein the X-ray source is at a fixed position.

- **Primary optics**

  Special optical devices are used to which determines the form and size of X-Ray beam and to maximize intensity of the signal or accurately get the required wavelength. Single crystal monochromators are used to get a monochormatic beam of certain wavelengths, typically $K_{\alpha 1}$, by removing $K_{\alpha 2}$ and K_{β}. Monochromators, called as Gobel mirrors, are designed to parallelize the beam using multilayer coated optic systems. They are ideal for examining irregularly shaped samples requiring high beam intensity or angular resolution.
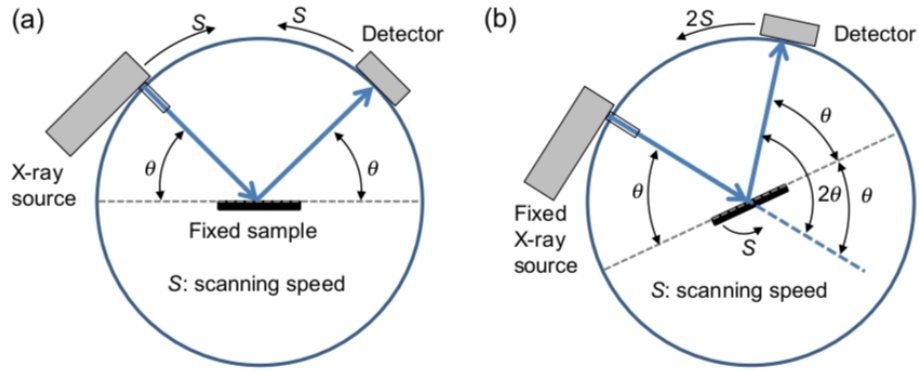
Figure 8: Two types of ganioneter

- **Secondary optics**

  These are positioned between sample and the detector which shape the diffracted beam. Components from the primary optics such as slit systems, are often used to decrease the beam divergence and to get sharp peaks at the expense of intensity.Secondary monochromators are utilized to eliminate the unwanted wavelengths, such as K_β radiation or fluorescence, for specific investigations.

- **Detectors**

  Various types of detectors are used to measure the intensity of diffracted beam. These operate by converting the incoming x-ray photons into a detectable signal. These detectors use different technology, the gas detectors rely on ionization of gas by the x-ray photons, which produce voltage pulses. Solid detectors use the floursence of special material, converting it into Voltage pulses or visible light Semiconductor detectors offer excellent energy resolution and are therefore commonly used in the energy-dispersive measurements.[15]

2.2.2 Impedence spectroscopy

In impedance spectroscopy AC impedance measurements are conducted across a broad range of frequencies and different sections of the materials are characterized based on their electrical relaxation time or time constants. Impedance spectroscopy is comparatively easy to use and can be applied to a broad range of materials and challenges.

Figure 9: AC Conductivity setup

- **Basic concepts of EIS**

  In a typical electrochemical cell, interactions between the matter, electrodes and the redox species has various process such as concentration of electroactive species, charge transfer and mass transfer which is from bulk surface to the electrode surface. These interactions contributes to the overall behaviour of the cell and can be studided using EIS. it allows for the exploration of mass transfer, charge transfer by representing them as electrical circuit elements like resistances, capacitors, or constant phase elements. These elements are then interconnected either in parallel or in series to form a equivalent circuit and can be used to study the properties of material such as capacitance, conductance or resistance. the impedence which is using EIS is different from the impedence measured by using a dc circuit because it posses

both resistance and reactance

The relation between the radial frequency (ω) and applied frequency(f) is calculated by equation [16]

$$\omega = 2\pi f$$

In linear system, signal is shifted in phase (ϕ) and has a different amplitude than I_0 given by the equation.

$$I_t = I_0 sin(\omega t + \phi)$$

Thus, the impedance of the whole system can be obtained from Equation:

$$Z = Z_0 exp(i\phi) = Z_0(cos\phi + isin\phi) \tag{1}$$

where Z, E, I, ω, and ϕ are impedance, potential, current, frequency, and phase shift between E and I respectively. There are two parts for the impedence expression an imaginary part Z_{imag} and a real part Z_{real}. A nyquist plot can be formed by plotting the real part on x axis and imaginary part on y axis. [16]

- **Theory**

  It involves measuring impedance of a sample across a broad frequency range, usually varying from low to high frequencies(10^{-2} TO 10^7)Hz. There are generally two components of impedence namely resistive and reactive both these components must be determined. One method involves applying an alternating voltage across the sample and a standard resistor in series. The in-phase and out-of-phase voltage components are measured across the sample, then it is divided by the current magnitude to extract resistive and reactive components.

  This process is repeated at different frequencies to characterize impedance across a frequency range. Materials often show an impedance spectrum characterized by two distinguishable

features arising from within the grains (bulk) and between grains (grain boundaries). For the
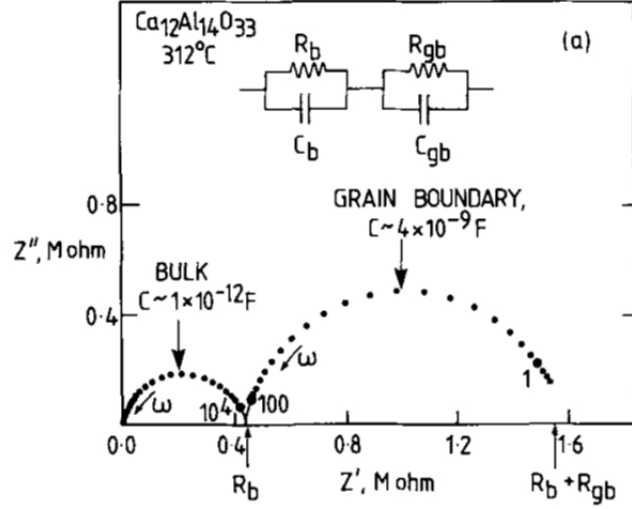
Figure 10: Impedance graph and equivalent circuit[16]

oxide ion conductor $Ca_{12}Al_{14}O_{33}$, impedance data is presented in a plot where imaginary (Z")
and real (Z impedances are shown. Each parallel RC element, represented by two semicircles,
which results in a semicircular pattern. Ideally, the component values of resistance (R) are
derived from the intercepts on the Z' axis, while the capacitance (C) values are determined
by applying equation

$$\omega_{max} RC = 1$$

to the frequency at the peak of each semicircle. After finding the R and C components next
step is to find which region of sample is assigned to them The assesment depends upon the
magnitudes of capacitances outlined in figure 11 . In the case of a parallel plate capacitor
with area A, separation 1 between plates, and a medium of permittivity E' between them,
the capacitance is determined by Equation

$$C = \epsilon' e_0 \frac{A}{l}$$

20

Capacitance [F]	Phenomenon Responsible
10^{-12}	bulk
10^{-11}	minor, second phase
10^{-11}–10^{-8}	grain boundary
10^{-10}–10^{-9}	bulk ferroelectric
10^{-9}–10^{-7}	surface layer
10^{-7}–10^{-5}	sample-electrode interface
10^{-4}	electrochemical reactions

Figure 11: Capacitance values and their possible interpretation[16]

The high-frequency semicircle shown in the Figure 10 exhibits a capacitance of a similar magnitude. Therefore, this semicircle, along with its corresponding resistance, is due to bulk characteristics of the sample and the other semicircle is due to grain boundary capacitance.[16]

2.2.3 DC Polarization

DC polarization technique was used to find the ionic transference number. Firstly pellets were sintered at 1260°C and silvercoated with silver paste to establish electrical contact. Then these pellets were placed in a oven at 500 °C so that the organic compound which was used as adhesive gets vaporised or else it could decrease the ionic conductivity.

Figure 12: Dc conductivity setup

A constant voltage of 0.8 V was applied across the sample and the current response was measured with respect to time, current readings were measured until the current readings becomes stable. Then to find the ionic transference number a graph of current v/s time was plotted. Here are some instruments used

- **DC power supply**
  Scientech 4072 DC power supply is designed as constant current and constant voltage source which can be used in laboratories. In this instrument a three digit display for voltage and current is used it was used to provide constant voltage.

- **Electrometer** Keithley model 6514 system electrometer was used to measure the current.

3   Results and Analysis

3.1   Identification of phase using power XRD

The parent sample and Nb doped sample was prepared having composition $N_{3.4}Zr_2Si_{2.4}P_{0.6}O_{12}$ and $N_{3.3}Nb_{0.1}Zr_{1.9}Si_{2.4}P_{0.6}O_{12}$ by using solution assisted solid state technique and the XRD data of the samples was collected. The data was measured at room temperature and the θ between which the sample was scanned was 10-80°. A 10 minute scan was performed with the scan speed being 5° per minutes. Using a CuK_α a radiation which has a wavelength of 1.54 A It was observed in the first attempt the phase formation in the parent sample was proper but the concentration of impurity phases (ZrO_2) was very high. This phenomenon could occur if the zirconium dioxide (ZrO_2) impurity wasn't removed during calcination

Then we increased the calcination time from 5 hr to 12 hr and Xrd data was collected of this
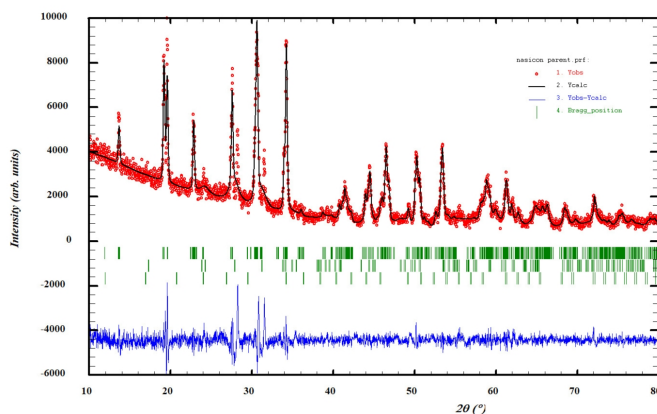
Figure 13: Parent sample Xrd plot

sample. As we can see from the XRD plot the phases were properly formed and the concentration of impurity is also acceptable. We tried to do reitveld refinment for this data but the χ^2 value was coming very high therefore we used le bail fitting for this data.

The major parent phase peak were seen at 19○, 31○, and 33° and a monoclinic phase had formed with a space group C2/c. There were two main impurity phases present which were ZrO_2 and Na_3PO_4. Then Xrd data of Nb doped sample was collected by using same diffractometer . The
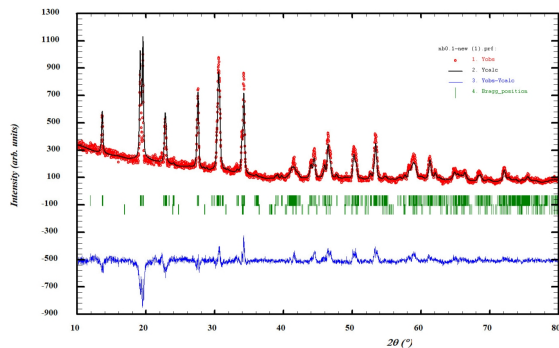
Figure 14: Nb-doped sample Xrd plot

data was then refined using reitveld refinement and a χ^2 value of 3.125 was obtained. Only one impurity phase was found in this. From the output file we come to know that the main phase was 99.51 percent present and the impurity phase was 0.49 percent . It's main phase peak position were 19°, 31° and 33°. A monoclinic phase was formed which had a space group C2/c. Thus from the Xrd plots we can conclude that the phases of both the samples were properly formed and the parent sample had more impurity phases than the Nb doped sample.

	a	b	c	α	β	γ
Nb doped main phase	15.69	9.07	9.20	90	124	90
Parent main phase	15.71	9.06	9.24	90	123.94	90

Table 1: Lattice parameters of both samples

24

3.2 AC conductivity measurements

Impedence spectroscopy (AC conductivity) was used to find the ionic conductivity of the two samples. The Impedence spectroscopy data was recorded for the parent sample ($Na_{3.4}Zr_2Si_{2.4}P_{0.6}O_{12}$) and Niobioum ($Na_{3.3}Nb_{0.1}Zr_2Si_{2.3}P_{0.6}O_{12}$) doped sample at room and high temperature by using the pallets sintered at 1260 °C made from these samples and after silver pasting them.

Figure 15: Measurement of impedence data of sintered pallet

The silverpasted pellets were then kept in oven for 2 hr at 500 °C which evaporates the organic compounds present in the silverpaste which is used as adhesive or else it can lower the ionic conductivity while measuring. Then impedance data for both the samples were recorded for a Freq range between 10 hz to 8 Mhz, with the help of this data a Nyquist plot was plotted.

Here is Nyquist plots of both the samples at room temperature As we can see from the Nyquist plot the sample Niobium doped sample has significantly less bulk as well as grain boundary impe-
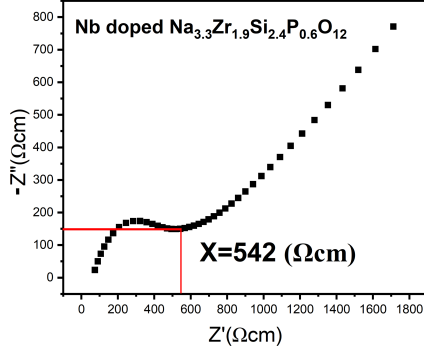
Figure 16: Nyquist plot of Nb doped sample
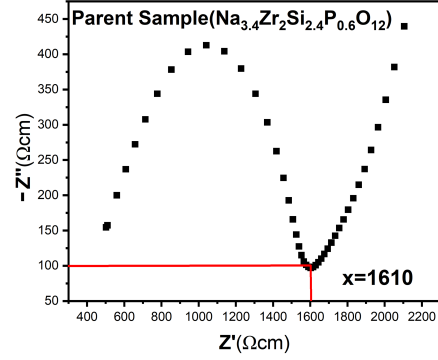
Figure 17: Nyquist plot of parent sample

dence. The ionic conductivity of both the samples were calculated with the help of formula

$$\sigma = \frac{1}{R_{total}} \times \frac{l}{A}$$

where l, A, and $R_t$otal represent thickness of pellet, Area of pellet and total impedence respectively. The ionic conductivity of parent sample at room temperature was found to be 0.625 mS cm^{-1} and Niobium doped sample was 1.9 mScm^{-1} respectively
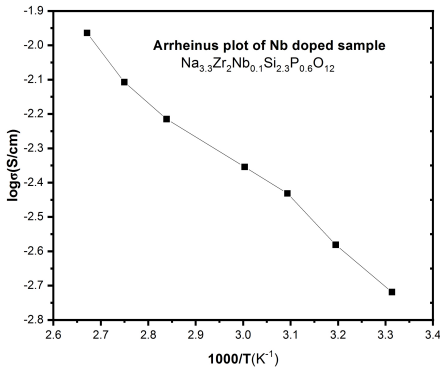
Figure 18: Arrhenius plot of Nb doped sample
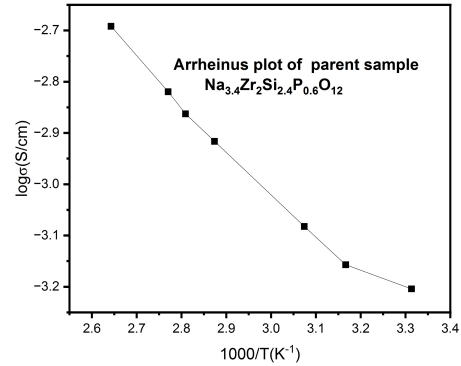
Figure 19: Arrhenius plot of parent sample

The arrhenius graph of conductivity data was plotted from 30 °C to 100 °C and as we can see as the temperature increases the ionic conductivity also increases linearly

Temperature (c)	Parent sample conductivity ($mScm^{-1}$)	Nb-doped sample conductivity ($mScm^{-1}$)
29	0.625	1.9
50	0.9	3.9
90	1.6	7.8

Table 2: Conductivity at different temperatures

The total ionic conductivity of Nb-doped sample is compared with other NASICON materials. $Na_3Zr_2Si_2PO_{12}$ has been playing an important role as a benchmark for many NASICON solid-state electrolyte materials which has a room temperature ionic conductivity of $\sigma > 10^{-4} Scm^{-1}$.

Different methods have been tried to enhance the ionic conductivity of the nasicon electrolyte. As we can see from our analysis there is a good increase in the ionic conductivity after doping the sample with niobium as the ionic conductivity increases from 0.625 to 1.9 m S cm^{-1}.[8]

3.3 DC conductivity measurements

DC conductivity measurements of the two samples were carried out. Firstly the pallets were silver pasted on both sides to provide electrical contact and then they were kept in oven at 500°C for 2 h so that the organic compound get vaporised. Then a voltage of 0.8 v was applied and current

Figure 20: Silver pasted pellets

was noted down, then a graph of current v/s time was plotted. The current readings were taken for an hour and from the graph of current v/s time we find the ionic transference number. The ionic transference number is very important as it tells us about the total conductivity of the sample and contribution of ionic conductivity. Ionic Transference number close to one is desired for a
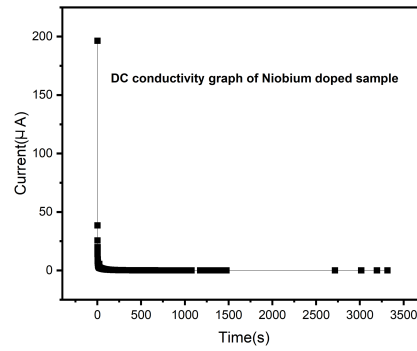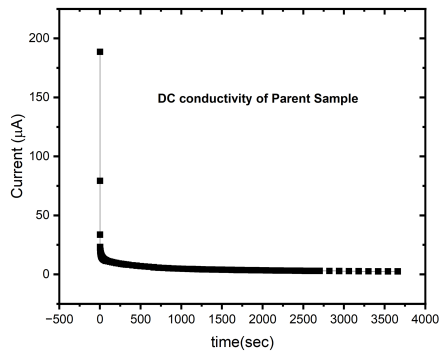
Figure 21: DC conductivity of parent sample

Figure 22: DC conductivity of Nb doped sample

electrolyte material as it shows that maximum conductivity is due to the ionic conductivity which is important for an electrolyte material. The formula used to find the ionic transference number is

Ionic transference number$=\frac{\text{Highest value of current} - \text{Constant current value}}{\text{Highest current value}}$

The ionic transference number was calculated for the parent and niobium doped sample sample using this formula which was 0.98 for parent sample and 0.99 for niobium doped sample.

4 Conclusion

A NASICON-type solid electrolyte $Na_{3.4}Zr_2Si_{2.4}P_{0.6}O_{12}$ (NZSP) was prepared by a solution-assisted solid-state reaction method. It was doped with niobium and we saw that the ionic conductivity of the doped sample had increased to 1.9 mScm^{-1}. Lower grain boundary resistance suggests that adding Niobium (Nb) aided the sintering process of NZSP. This resulted in denser electrolyte materials, likely due to increased phase purity and minimal presence of impurities like Zirconium dioxide (ZrO_2). The decrease in overall impedance is potentially caused by a combination of factors: higher sodium ion concentration and the influence of Nb^{5+} ions on the local structure of the material.

References

[1] Jianmin Ma, Yutao Li, Nicholas S Grundish, John B Goodenough, Yuhui Chen, Limin Guo, Zhangquan Peng, Xiaoqun Qi, Fengyi Yang, Long Qie, Chang-An Wang, Bing Huang, Zeya Huang, Linhui Chen, Dawei Su, Guoxiu Wang, Xinwen Peng, Zehong Chen, Junliang Yang, Shiman He, Xu Zhang, Haijun Yu, Chaopeng Fu, Min Jiang, Wenzhuo Deng, Chuan-Fu Sun, Qingguang Pan, Yongbing Tang, Xianfeng Li, Xiulei Ji, Fang Wan, Zhiqiang Niu, Fang Lian, Caiyun Wang, Gordon G Wallace, Min Fan, Qinghai Meng, Sen Xin, Yu-Guo Guo, and Li-Jun Wan. The 2021 battery technology roadmap. *Journal of Physics D: Applied Physics*, 54(18):183001, feb 2021.

[2] Naoki Nitta, Feixiang Wu, Jung Tae Lee, and Gleb Yushin. Li-ion battery materials: present and future. *Materials Today*, 18(5):252–264, 2015.

[3] Dongsheng Geng, Ning Ding, T. S. Andy Hor, Sheau Wei Chien, Zhaolin Liu, Delvin Wuu, Xueliang Sun, and Yun Zong. From lithium-oxygen to lithium-air batteries: Challenges and opportunities. *Advanced Energy Materials*, 6(9):1502164, 2016.

[4] Vincenzo Caramia and Benedetto Bozzini. Materials science aspects of zinc–air batteries: a review. *Materials for Renewable and Sustainable Energy*, 3(2):1–12, 2014.

[5] Shyamal K. Das, Sadhan Mahapatra, and Homen Lahan. Aluminium-ion batteries: developments and challenges. *J. Mater. Chem. A*, 5:6347–6367, 2017.

[6] Yumei Wang, Shufeng Song, Chaohe Xu, Ning Hu, Janina Molenda, and Li Lu. Development of solid-state electrolytes for sodium-ion battery–a short review. *Nano Materials Science*, 1(2):91–100, 2019.

[7] Yogesh Singh, Rahul Parmar, Mamta, Sanju Rani, Manoj Kumar, Kamlesh Kumar Maurya, and Vidya Nand Singh. Na ion batteries: An india centric review. *Heliyon*, 8(8):e10013, 2022.

[8] Yujian Liu, Limin Liu, Jinsong Peng, Xiaoliang Zhou, Dongshi Liang, Lei Zhao, Jiawen Su, Bo Zhang, Si Li, Naiqing Zhang, Qianli Ma, and Frank Tietz. A niobium-substituted sodium

superionic conductor with conductivity higher than 5.5 ms cm-1 prepared by solution-assisted solid-state reaction method. *Journal of Power Sources*, 518:230765, 2022.

[9] Chi Li, Rui Li, Kaining Liu, Rui Si, Zhizhen Zhang, and Yong-Sheng Hu. Nasicon: A promising solid electrolyte for solid-state sodium batteries. *Interdisciplinary Materials*, 1(3):396–416, 2022.

[10] L. Shen, J. Yang, G. Liu, M. Avdeev, and X. Yao. High ionic conductivity and dendrite-resistant nasicon solid electrolyte for all-solid-state sodium batteries. *Materials Today Energy*, 20:100691, 2021.

[11] Lingbing Ran, Ardeshir Baktash, Ming Li, Yu Yin, Baris Demir, Tongen Lin, Meng Li, Masud Rana, Ian Gentle, Lianzhou Wang, Debra Searles, and Ruth Knibbe. Sc, ge co-doping nasicon boosts solid-state sodium ion batteries' performance. *Energy Storage Materials*, 40, 05 2021.

[12] Herbert Schmid, Lutgard C. De Jonghe, and Craig Cameron. Chemical stability of nasicon. *Solid State Ionics*, 6(1):57–63, 1982.

[13] Lixiao Zhang, Yimeng Liu, Ya You, Ajayan Vinu, and Liqiang Mai. Nasicons-type solid-state electrolytes: The history, physicochemical properties, and challenges. *Interdisciplinary Materials*, 2(1):91–110, 2023.

[14] Andrei A. Bunaciu, Elena UdriŞTioiu, and Hassan Aboul-Enein. X-ray diffraction: Instrumentation and applications. *Critical reviews in analytical chemistry / CRC*, 45, 04 2015.

[15] Andrei A. Bunaciu, Elena UdriŞTioiu, and Hassan Aboul-Enein. X-ray diffraction: Instrumentation and applications. *Critical reviews in analytical chemistry / CRC*, 45, 04 2015.

[16] Hend S. Magar, Rabeay Y. A. Hassan, and Ashok Mulchandani. Electrochemical impedance spectroscopy (eis): Principles, construction, and biosensing applications. *Sensors*, 21(19), 2021.